# Realization of Current Mode Universal Filter and a Dual-Mode Single Resistance Controlled Quadrature Oscillator Employing VDCC and Only Grounded Passive Elements

*Manish GUPTA*[1], *Tajinder Singh ARORA*[2]

[1]Department of Electronics and Communication Engineering, Inderprastha Engineering College, Surya Nagar Flyover Road, Ghaziabad, 201004 Uttar Pradesh, India
[2]Department of Electronics and Communication Engineering, Maharaja Surajmal Institute of Technology, Lal Sain Mandir Marg, Janakpuri, 110058 New Delhi, India

guptamanish2004@gmail.com, tajarora@gmail.com

DOI: 10.15598/aeee.v15i5.2397

***Abstract.*** *The manuscript presents a circuit that can act as a universal filter as well as a single resistance controlled oscillator by unpretentiously changing the switch positions. The circuit employs only two active devices and all grounded passive elements. The utilization of only grounded passive components makes this circuit a better choice for integrated circuit implementation. The current mode biquadratic filter offers all the five basic responses along with independent tunability of its quality factor. The dual-mode quadrature sinusoidal oscillator offers explicit current outputs along with voltage outputs. The circuit also offers a simple and uncoupled condition of oscillation and frequency of oscillation. The typical analysis such as non-ideal, sensitivity and parasitic analysis along with the regular simulation results as well as experimental results are exposed here, to strengthen the design idea.*

## Keywords

***Current Mode circuits, single resistance controlled oscillator, universal filter, voltage differencing current conveyor.***

## 1. Introduction

From last few decades, there has been a predominance of digital signal processing over analog signal processing. But this does not pose any threat to it; rather it gave more challenges and opportunity to the designer and researcher of analog circuits. Analog signal processing, where natural/ analog signals are handled as per the specifications, has its own advantages such as higher bandwidth, faster speed of operation etc. In the domain of analog circuits, some of the most widely employed applications are active filters, sinusoidal oscillator, non-linear waveforms generator, synthetic inductor realization [1], [2], [3], [4] and [5]. Frequency selective filters and sinusoidal oscillator, since long, have found impeccable application in communication receiver, control systems etc. [6]. Frequency selective filters, as the name implies, is the block that passes /attenuates any specific frequency or a band of frequencies whereas oscillator is a circuit that generates the undamped waveform of any designed frequency.

The reference no. [7] exposed a gateway to the upcoming future devices; Voltage Differencing Current Conveyor (VDCC) is one of them. So many applications of this active device [8], [9], [10], [11], [12], [13], [14], [15], [16], [17], [18], [19], [20], [21] and [22], and references cited therein, are made available in the open literature. But still as per authors' perception, this active device has to be much more explored and exploited for analog signal processing applications, in future.

Out of these [8], [9], [10], [11], [12], [13], [14], [15], [16], [17], [18], [19], [20], [21] and [22], synthetic inductor is realized in [8], [9] and [10], passive element simulator in [11] and [12], active filter was presented in [13], [14], [15], [16] and [17], and sinusoidal oscillator in [18], [19], [20] and [21]. The behavioral model of the active device is discussed in detail in [22]. Comparison of the designed universal filter circuit with the earlier work done on VDCC based filters is as follows. In [13] a voltage mode universal active filter using single

**Tab. 1:** Comparison table of literature survey (Active Filter).

| Ref. No. | Mode of operation | All five types of responses available | Number of VDCC employed | Number of passive elements used | Whether all passive elements grounded | Matching of impedances at input and output level | Is $Q_0$ independently tunable |
|---|---|---|---|---|---|---|---|
| [13] | Voltage mode | Yes | 1 | 3 | No | No | No |
| [14] | Current mode | Yes | 1 | 3 | Yes | No | No |
| [15] | Current mode | Yes | 2 | 4 | Yes | No | Yes |
| [16] | Voltage mode | No | 2 | 7 | No | No | Yes |
| Proposed circuit | Current mode | Yes | 2 | 4 | Yes | Yes | Yes |

**Tab. 2:** Comparison table of literature survey (Sinusoidal Oscillator).

| Ref. No. | Number of VDCC employed | Whether all passive elements grounded | Non-interacting CO and FO | Availability of explicit quadrature outputs | Is operation in CM/VM both mode | Any significant remarks |
|---|---|---|---|---|---|---|
| [18] | 1 | Yes | No | No | No | Availability of BP and LP responses in transconductance mode |
| [19] | 2 | Yes | Yes | Yes | Yes | - |
| [20] | 1 | Yes | No | Yes | No | Multiphase Oscillator (Linear Control of FO) |
| [21] | 1 | Yes | No | Yes | No | - |
| Proposed circuit | 2 | Yes | Yes | Yes | Yes | Availability of current mode Universal filter |

VDCC is presented but it suffers from the drawback of the utilization of floating passive elements. A current mode universal filter with less number of active devices is presented in [14] but the circuit has a drawback that the filter parameters are not independently tunable. The circuit given in [15] uses the same number of active and passive devices but input current is not injected at low impedance port. Additionally, circuit can perform one function only. In [16] higher numbers of passive elements were used. First ever, first order all-pass filter using single VDCC is presented in [17]. A qualitative comparison of parameters with given literature survey is shown in Tab. 1.

Now the comparison of the proposed oscillator with the earlier published work is given as follows. The quadrature oscillator, employing all grounded passive elements, which is not having non-interacting CO and FO (also known as fully uncoupled) and its tuning capability is limited with passive grounded element only, is presented in [18] and [21]. In [19], the same number of active and passive elements are utilized, but works as a sinusoidal oscillator only (can't perform the function of active filter). In [20], a multiphase oscillator using controlled gain VDCC was proposed but requires a matching condition to the linear control of oscillation frequency. A comparative analysis is also presented in Tab. 2.

The purpose of this manuscript is to present one such circuit that can work as a universal filter along with a sinusoidal oscillator. In conclusion, the circuit offers various features, when used as an active filter, such as:

- Availability of all five responses in current mode i.e. low pass, high pass, band pass, band reject and all pass filter function.
- Independent tunability of its quality factor ($Q_0$).
- Orthogonal tunability of its center frequency ($\omega_0$).
- Availability of explicit current output.
- Use of only grounded passive elements.
- Availability of low impedance at input port and high impedance at output port.

Whereas when the same circuit acts as sinusoidal oscillator reflects some useful characteristics e.g.

- Availability of explicit current output.
- Use of only grounded passive elements.
- Availability of quadrature current output (explicit).
- Availability of voltage mode quadrature output.
- Simple Condition of Oscillation (CO) and Frequency of Oscillation (FO).
- Uncoupled CO and FO.
- FO can be tuned either electronically or by use of grounded passive resistor.
- CO can also be adjusted by grounded passive resistor or by electronic tunability.

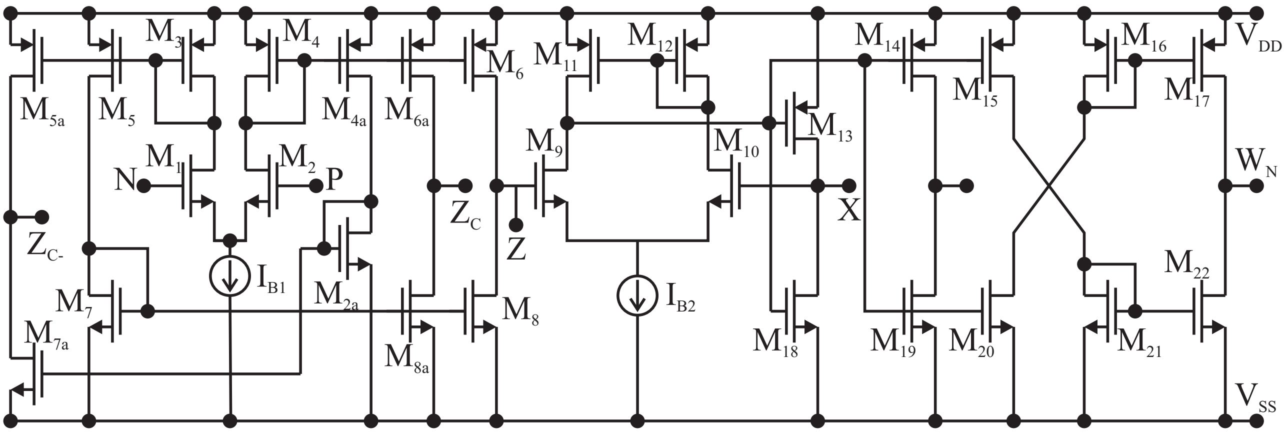


**Fig. 1:** MOS realization of the Voltage Differencing Current Conveyor [15].

Full manuscript is divided into five main sections. At the outset, the present section gives the introduction of analog signal processing and comparison between previous work and presented work. Section 2. presents the active device i.e. VDCC along with the proposed circuit. Non-ideal and sensitivity analysis is depicted in Sec. 3. . Section 4. states the effects of parasitic of the active device under consideration, on the proposed circuit. To verify the theoretical analysis, Sec. 5. contains all the simulation results. Experimental results are given in Sec. 6. At last, conclusion is provided in Sec. 7.

## 2. Proposed Circuit

The electrical combination of an Operational Transconductance Amplifier (OTA) and a second generation Current Conveyor (CCII) is known as VDCC. The block diagram along with its functional circuit diagram, employing CMOS transistors, are shown in Fig. 2 and Fig. 1 respectively. Equation (1) represents the natural characteristics of the active device. Here $g_m$ is the transconductance factor of the device; additionally, this is electronically tunable with the help of the bias current i.e. $I_{B1}$ (Fig. 2).

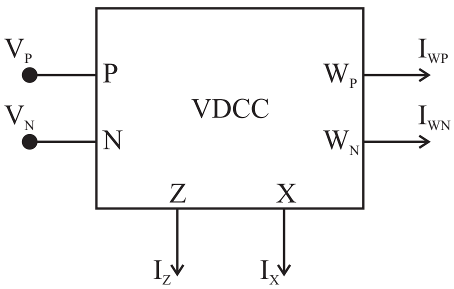


**Fig. 2:** Block Diagram of VDCC [8].

$$
\begin{bmatrix} I_P \\ I_N \\ I_Z \\ V_X \\ I_{WP} \\ I_{WN} \end{bmatrix} = \begin{bmatrix} 0 & 0 & 0 & 0 \\ 0 & 0 & 0 & 0 \\ g_m & -g_m & 0 & 0 \\ 0 & 0 & 1 & 0 \\ 0 & 0 & 0 & 1 \\ 0 & 0 & 0 & -1 \end{bmatrix} \begin{bmatrix} V_P \\ V_N \\ V_Z \\ I_X \end{bmatrix}. \quad (1)
$$

The proposed circuit that can work as a current mode universal filter, as well as single resistance controlled oscillator, by simply altering the switch position, is shown in Fig. 3. Table 3 shows the basic combination of switches, as shown in Fig. 3, so that the circuit can provide the desired nature of the operation.

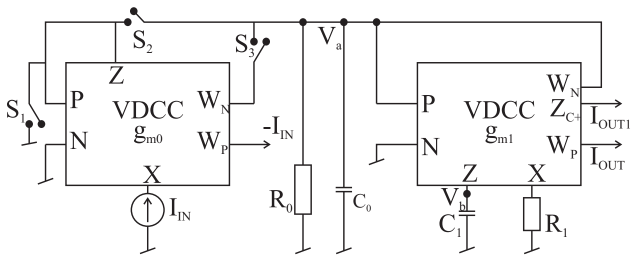


**Fig. 3:** Proposed realization of filter cum Oscillator Circuit.

**Tab. 3:** Characteristic table (for the circuit shown in Fig. 3).

| S. No. | Switches | | | Operation |
|---|---|---|---|---|
| | S1 | S2 | S3 | |
| 1. | ON | OFF | ON | Current mode universal filter |
| 2. | OFF | ON | OFF | Dual mode quadrature oscillator |

When the switch combination as given in S.No. 1 of Tab. 3 is applied, the circuit behaves as an active filter. To get all the desired transfer functions, we simply apply the basics of circuit theory on the Fig. 3, utilizing the characteristic equation of VDCC i.e. given in Eq. (1). All five desired transfer function of a universal filter i.e. low pass, high pass, band pass, band stop and all pass are presented in Eq. (2), Eq. (3), Eq. (5), Eq. (7) and Eq. (9). The common denominator polynomial, expression for the center frequency and quality factor are given by Eq. (10), Eq. (11) and Eq. (12). It is evident from Eq. (12) that the $Q_0$ is independent of $\omega_0$ and its value can be varied by varying a grounded passive resistor i.e. $R_0$. The gain of the given Band Pass ($H_{BP}$) and Low Pass ($H_{LP}$) filter function is given in Eq. (13).

$$\frac{I_{OUT1}}{I_{IN}} = \frac{I_{BP}}{I_{IN}} = \frac{\frac{s \cdot g_{m1}}{C_0}}{D(s)}. \tag{2}$$

$$\frac{I_{OUT}}{I_{IN}} = \frac{I_{LP}}{I_{IN}} = \frac{\frac{g_{m1}}{R_1 C_0 C_1}}{D(s)}. \tag{3}$$

If $g_{m1} R_0 = 1$,

$$I_{HP} = -I_{IN} + I_{BP} + I_{LP}, \tag{4}$$

$$\frac{I_{HP}}{I_{IN}} = -\frac{s^2}{D(s)}. \tag{5}$$

$$I_{BS} = I_{HP} - I_{BP}, \tag{6}$$

$$\frac{I_{BS}}{I_{IN}} = -\frac{s^2 + \frac{s}{R_0 C_0}}{D(s)}. \tag{7}$$

$$I_{AP} = -I_{HP} - I_{BP} + I_{LP}, \tag{8}$$

$$\frac{I_{AP}}{I_{IN}} = \frac{s^2 - \frac{s}{R_0 C_0} + \frac{g_{m1}}{R_1 C_0 C_1}}{D(s)}. \tag{9}$$

$$D(s) = s^2 + \frac{s}{R_0 C_0} + \frac{g_{m1}}{R_1 C_0 C_1}. \tag{10}$$

$$\omega_0 = \sqrt{\frac{g_{m1}}{R_1 C_0 C_1}}. \tag{11}$$

$$Q_0 = R_0 \sqrt{\frac{g_{m1} C_0}{R_1 C_1}}. \tag{12}$$

$$\left. \begin{array}{l} H_{LP} = 1 \\ H_{BP} = g_{m1} R_0 \end{array} \right\}, \tag{13}$$

where $\omega_0$ is the center frequency in rad·s$^{-1}$ and $Q_0$ is the quality factor.

When the appropriate switch combination of Tab. 3 (S.No.2) is applied, the proposed circuit works as a Single Resistance Controlled Oscillator (SRCO). The characteristic equation of the proposed SRCO is given by Eq. (14). The Condition of Oscillation (CO) and Frequency of Oscillation (FO) are simple and uncoupled to each other, represented by Eq. (15) and Eq. (16) respectively. Here, it is evident that the CO, as well as FO, can be tuned electronically ($g_{m0}$ for CO and $g_{m1}$ for FO) as well as with the help of grounded passive resistor ($R_0$ for CO and $R_1$ for FO), without affecting each other. The circuit offers two explicit current outputs that are in 90° phase shift to each other. These two quadrature outputs are $I_{OUT}$ and $I_{OUT1}$; namely. The relationship between them is shown by Eq. (17). Here it is worth noting that the derived circuit can also offer quadrature voltage outputs $V_a$ and $V_b$. The relationship between the both is justified by Eq. (18).

$$s^2 + \frac{s}{C_0}\left(\frac{1}{R_0} - g_{m0}\right) + \frac{g_{m1}}{R_1 C_0 C_1} = 0. \tag{14}$$

$$\text{C.O.} \quad \left(\frac{1}{R_0} - g_{m0}\right) = 0. \tag{15}$$

$$\text{F.O.} \quad \omega_0 = \sqrt{\frac{g_{m1}}{R_1 C_0 C_1}}. \tag{16}$$

$$\frac{I_{OUT}}{I_{OUT1}} = \frac{1}{s C_1 R_1}. \tag{17}$$

$$\frac{V_b}{V_a} = \frac{g_{m1}}{s C_1}. \tag{18}$$

## 3. Non-Ideal and Sensitivity Analysis

The deviation between ideal and non-ideal values of the active device can be checked through its given mathematical equation. Equation (19) represents the characteristics equations of VDCC where '$i$' represents the number of the active device that could be 0 and 1. The non-ideal factors are defined as $\alpha$, $\beta$, $\gamma_P$ and $\gamma_N$. The ideal values of $\alpha$, $\beta$, $\gamma_P$ and $\gamma_N$ are in unity only.

$$\left. \begin{array}{l} I_Z = \alpha_i \cdot g_{mi}(V_P - V_N) \\ V_X = \beta_i \cdot V_Z \\ I_{WP} = \gamma_{Pi} I_X \\ I_{WN} = -\gamma_{Ni} I_X \end{array} \right\}. \tag{19}$$

When Eq. (19) is used for analyzing the proposed circuit, as given in Fig. 3, by circuit theory fundamentals, non-ideal transfer functions are obtained. Equation (20) and Eq. (21) represent the transfer functions of band pass and low pass filters, whereas, frequency and qualify factor along with common denominator polynomial are given by Eq. (22), Eq. (23) and Eq. (24).

$$\frac{I_{OUT1}}{I_{IN}} = \frac{\alpha_1 \cdot \gamma_{NO}\left(\frac{s g_{m1}}{C_0}\right)}{D'(s)}. \tag{20}$$

$$\frac{I_{OUT}}{I_{IN}} = \frac{\alpha_1 \cdot \beta_1 \cdot \gamma_{P1} \cdot \gamma_{NO}\left(\frac{g_{m1}}{C_0 C_1 R_1}\right)}{D'(s)}. \tag{21}$$

$$\omega_0' = \sqrt{\frac{\alpha_1 \cdot \beta_1 \cdot g_{m1} \cdot \gamma_{N1}}{C_0 C_1 R_1}}. \tag{22}$$

$$Q_0' = R_0 \sqrt{\frac{C_0 \alpha_1 \cdot \beta_1 \cdot g_{m1} \cdot \gamma_{N1}}{C_1 R_1}}. \tag{23}$$

$$D'(s) = s^2 + s\left(\frac{1}{C_0 R_0}\right) + \frac{\alpha_1 \cdot \beta_1 \cdot \gamma_{N1} g_{m1}}{C_0 C_1 R_1}. \tag{24}$$

While doing the non-ideal analysis for the proposed sinusoidal oscillator, we get the following characteristic equation, given by Eq. (25). From Eq. (25), non-ideal CO and FO can be easily deduced, which are represented in Eq. (26) and Eq. (27) respectively.

$$s^2 + \frac{s}{C_0}\left(\frac{1}{R_0} - \alpha_0 \cdot g_{m0}\right) + \frac{\alpha_1 \cdot \beta_1 g_{m1} \gamma_{N1}}{R_1 C_0 C_1} = 0. \tag{25}$$

$$\text{C.O.} \quad \left(\frac{1}{R_0} - \alpha_0 \cdot g_{m0}\right) \geq 0. \tag{26}$$

$$\text{F.O.} \quad \omega_0 = \sqrt{\frac{\alpha_1 \cdot \beta_1 \cdot g_{m1} \gamma_{N1}}{R_1 C_0 C_1}}. \tag{27}$$

Sensitivity analysis was also carried out for both the proposed applications of VDCC. The sensitivity equations for the derived current mode universal filter are given by Eq. (28), Eq. (29), Eq. (30), Eq. (31), Eq. (32) and Eq. (33) and for SRCO derived sensitivity equations are represented by Eq. (34) to Eq. (35). All the derived sensitivity figures are under considerable limits.

$$S_{\alpha_1}^{\omega_0'} = S_{\beta_1}^{\omega_0'} = S_{\gamma_{N1}}^{\omega_0'} = \frac{1}{2}. \tag{28}$$

$$S_{g_{m1}}^{\omega_0'} = \frac{1}{2}; \quad S_{R_1}^{\omega_0'} = S_{C_1}^{\omega_0'} = S_{C_0}^{\omega_0'} = -\frac{1}{2}. \tag{29}$$

$$S_{\alpha_1}^{Q_0'} = S_{\beta_1}^{Q_0'} = S_{\gamma_{N1}}^{Q_0'} = \frac{1}{2}. \tag{30}$$

$$S_{g_{m1}}^{Q_0'} = S_{C_0}^{Q_0'} = \frac{1}{2}. \tag{31}$$

$$S_{C_1}^{Q_0'} = S_{R_1}^{Q_0'} = -\frac{1}{2}. \tag{32}$$

$$S_{R_0}^{Q_0'} = 1. \tag{33}$$

$$S_{\alpha_1}^{\omega_0'} = S_{\beta_1}^{\omega_0'} = S_{\gamma_{N1}}^{\omega_0'} = \frac{1}{2}. \tag{34}$$

$$S_{g_{m1}}^{\omega_0'} = \frac{1}{2}; \quad S_{R_1}^{\omega_0'} = S_{C_1}^{\omega_0'} = S_{C_0}^{\omega_0'} = -\frac{1}{2}. \tag{35}$$

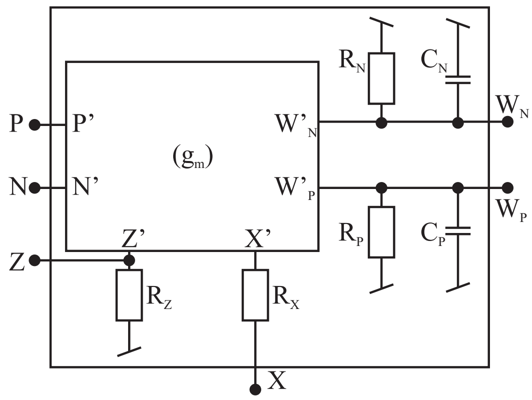


**Fig. 4:** Parasitic model of VDCC [19].

## 4. Parasitic Analysis

A well known parasitic model of VDCC [19] has been taken into consideration, shown in Fig. 4, to explore the effect of parasitic on designed circuits.

The next scheme shows the proposed circuit including parasitic effects. It is evidently shown that the proposed current mode universal filter and sinusoidal oscillator reflects good performance under the influence of parasitic.

### 4.1. Parasitic Analysis for Universal Filter

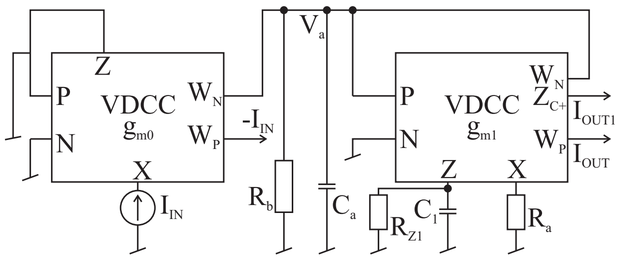


Assumptions:

$$R_a = R_1 + R_{X1}.$$

$$R_b = R_0 || R_{N0} || R_{N1}.$$

$$C_a = C_0 + C_{N0} + C_{N1}.$$

$$I_{OUT1} = \frac{\left[\frac{1}{R_{Z1}} + sC_1\right] \frac{g_{m1}}{C_a C_1}}{\widetilde{D}(s)}.$$

$$I_{OUT} = \frac{\frac{g_{m1}}{R_a C_1 C_a}}{\widetilde{D}(s)}.$$

$$\widetilde{D}(s) = s^2 + s\left[\frac{1}{C_1 R_{Z1}} + \frac{1}{C_a R_b}\right] + \frac{1}{C_a C_1}\left[\frac{g_{m1}}{R_a} + \frac{1}{R_{Z1} R_b}\right].$$

$$\widetilde{\omega}_0 = \sqrt{\frac{1}{C_1 C_a}\left[\frac{g_{m1}}{R_a} + \frac{1}{R_{Z1} R_b}\right]}.$$

$$\widetilde{Q}_0 = \frac{1}{\left[\frac{1}{C_1 R_{Z1}} + \frac{1}{C_a R_b}\right]}\sqrt{\frac{1}{C_1 C_a}\left[\frac{g_{m1}}{R_a} + \frac{1}{R_{Z1} R_b}\right]}.$$

$$S_{C_1}^{\widetilde{\omega}_0} = S_{C_a}^{\widetilde{\omega}_0} = -\frac{1}{2}.$$

$$S_{R_a}^{\widetilde{\omega}_0} = -S_{g_{m1}}^{\widetilde{\omega}_0} = -\frac{1}{2}\frac{\frac{g_{m1}}{R_a C_1 C_a}}{\frac{1}{C_1 C_a}\left[\frac{g_{m1}}{R_a} + \frac{1}{R_{Z1} R_b}\right]}.$$

$$S_{R_b}^{\widetilde{\omega}_0} = -S_{R_{Z1}}^{\widetilde{\omega}_0} = -\frac{1}{2}\frac{\frac{1}{C_1 C_a R_{Z1} R_b}}{\frac{1}{C_1 C_a}\left[\frac{g_{m1}}{R_a} + \frac{1}{R_{Z1} R_b}\right]}.$$

### 4.2. Parasitic Analysis for Sinusoidal Oscillator

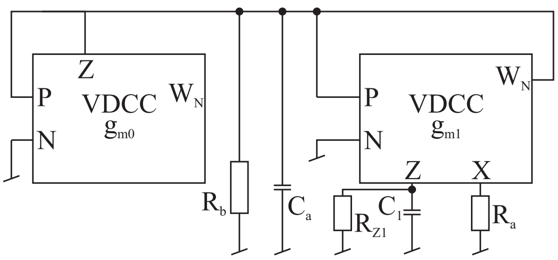


Assumptions:

$$R_a = R_1 + R_{X1}.$$

$$R_b = R_0 || R_{Z0} || R_{N1}.$$

$$C_a = C_0 + C_{N1}.$$

$$\text{CO:} \quad \frac{1}{C_a}[g_{m0} - R_b] = \frac{1}{C_1 R_{Z1}}.$$

$$\text{FO:} \quad \widetilde{\omega}_0^2 = \frac{1}{C_a C_1}\left[\frac{1}{R_{Z1}}\left(\frac{1}{R_b} - g_{m0}\right) + \frac{g_{m1}}{R_a}\right].$$

$$S_{C_1}^{\widetilde{\omega}_0} = S_{C_a}^{\widetilde{\omega}_0} = -\frac{1}{2}.$$

$$S_{R_a}^{\widetilde{\omega}_0} = -S_{g_{m1}}^{\widetilde{\omega}_0} = -\frac{1}{2}\frac{\frac{g_{m1}}{R_a C_1 C_a}}{\frac{1}{C_a C_1}\left[\frac{1}{R_{Z1}}\left(\frac{1}{R_b} - g_{m0}\right) + \frac{g_{m1}}{R_a}\right]}.$$

$$S_{R_b}^{\widetilde{\omega}_0} = -\frac{1}{2}\frac{\frac{1}{C_1 C_a R_{Z1} R_b}}{\frac{1}{C_a C_1}\left[\frac{1}{R_{Z1}}\left(\frac{1}{R_b} - g_{m0}\right) + \frac{g_{m1}}{R_a}\right]}.$$

$$S_{R_{Z1}}^{\widetilde{\omega}_0} = -\frac{1}{2}\frac{\frac{1}{C_1 C_a R_{Z1}}\left(\frac{1}{R_b} - g_{m0}\right)}{\frac{1}{C_a C_1}\left[\frac{1}{R_{Z1}}\left(\frac{1}{R_b} - g_{m0}\right) + \frac{g_{m1}}{R_a}\right]}.$$

$$S_{g_{m0}}^{\widetilde{\omega}_0} = -\frac{1}{2}\frac{\frac{g_{m0}}{R_{Z1} C_1 C_a}}{\frac{1}{C_a C_1}\left[\frac{1}{R_{Z1}}\left(\frac{1}{R_b} - g_{m0}\right) + \frac{g_{m1}}{R_a}\right]}.$$

## 5. Simulation Results

Feasibility of the proposed filter cum oscillator circuit, with all grounded passive components, has been tested and simulated using Cadence PSPICE simulation software. The CMOS version shown in Fig. 1, using 0.18 µm TSMC MOS process parameters [23], is utilized for generating the graphical results. The aspect ratios, used in Fig. 1, are presented in Tab. 4 [8]. For simulation, supply voltage of ±0.9 V and bias current of 50 µA ($I_{B1}$) and 100 µA ($I_{B2}$), shown in Fig. 1, are used and the corresponding value of transconductance gain ($g_m$) is 277 µA·V$^{-1}$. All the simulation results of the derived circuit are mainly divided into two parts - former depict universal filter's simulation results and latter shows the simulation graphs for the oscillator circuit.

For the testing of the universal filter, the passive components were selected as $R_0 = R_1 = 3.6$ kΩ, $C_0 = 21.9$ pF, $C_1 = 87.6$ pF and the transconductance gain of the active device is 277 µA·V$^{-1}$. Figure 5 demonstrates that the designed current mode circuit can be utilized as a low pass, high pass, band pass and band stop filter. Here the center frequency was chosen as 1 MHz and the value of the quality factor is 0.5. The proposed circuit can also act like an all pass filter whose gain as well as phase response is depicted in Fig. 6. Figure 5 and Fig. 6 collectively justify the design of a universal filter using VDCC with all grounded passive components. As given in Eq. (12), $Q_0$ can be varied with the help of resistance $R_0$ without altering the center frequency. So the variation of the quality factor by changing the value of grounded passive resistor $R_0$ is shown in Fig. 7. Table 5 gives the range of $R_0$ and their corresponding value of $Q_0$.

**Tab. 4:** Aspect ratios of the MOS devices [8].

| CMOS transistors | W/L (in μ/m) |
|---|---|
| M1–M4 | 3.6/1.8 |
| M5, M6 | 7.2/1.8 |
| M7, M8 | 2.4/1.8 |
| M9, M10 | 3.06/0.72 |
| M11, M12 | 9.0/0.72 |
| M13–M17 | 14.4/0.72 |
| M18–M22 | 0.72/0.72 |

**Tab. 5:** $Q_0$ tunability (passive Components values).

| $Q_0$ | $R_0$ (in kΩ) |
|---|---|
| 0.25 | 1.8 |
| 0.35 | 2.54 |
| 0.5 | 3.6 |
| 0.707 | 5.09 |
| 1 | 7.2 |
| 1.414 | 10.18 |

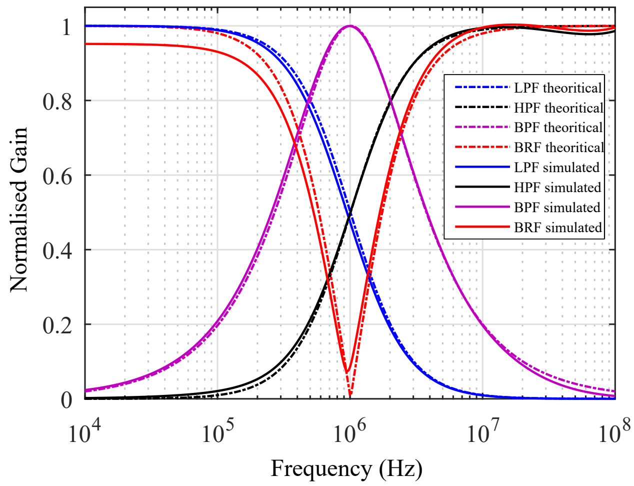


**Fig. 5:** Current mode filter responses of low pass, high pass, band pass and band reject functions.

Apart from $Q_0$ tunability, the center frequency of the designed filter can also be varied, as shown in Fig. 8. The passive elements values selected for Fig. 8 are given in Tab. 6. The transient response of the band pass filter is also simulated at 1 MHz, represented in Fig. 9. Figure 9 depicts that at input current of 25 μA, the output is distortion free. Total Harmonic Distortion (THD) of the designed current mode filter circuit is also calculated. The graph plotted between input current versus existing percentage of THD, is depicted in Fig. 10. Figure 10 shows that up to 80 μA of input current the THD is significantly low.

The proposed circuit can also be utilized as a single resistance controlled oscillator with all grounded components. The passive components values for the designed sinusoidal oscillator were chosen as $R_1 = 15$ kΩ, $C_0 = C_1 = 21.9$ pF and the transconductance gain of the active device is 277 μA·V$^{-1}$. The transient and the steady state responses, with explicit current output are shown in Fig. 11 and Fig. 12, respectively. Additionally, Fig. 12 represents the quadrature outputs in current mode. As discussed in Sec. 2. , the designed oscillator can also deliver the voltage mode quadrature output, represented in Fig. 13. Lissajous patterns for the current and voltage mode quadrature outputs are also plotted in Fig. 14 and Fig. 15, respectively. It can be seen from last two figures that there are no tilts in the ellipses, hence verifying the quadrature relation-

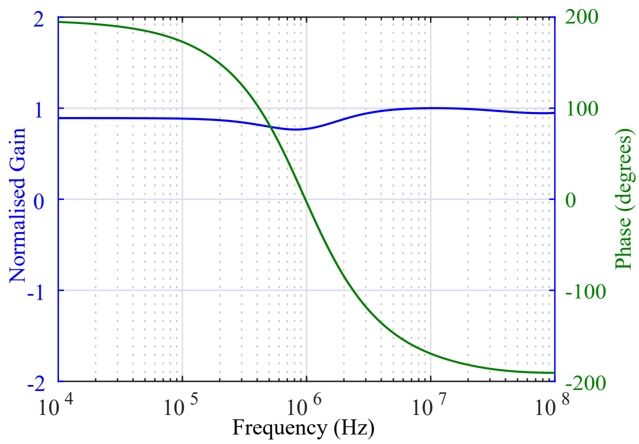


**Fig. 6:** Gain and phase response of an all pass filter function.

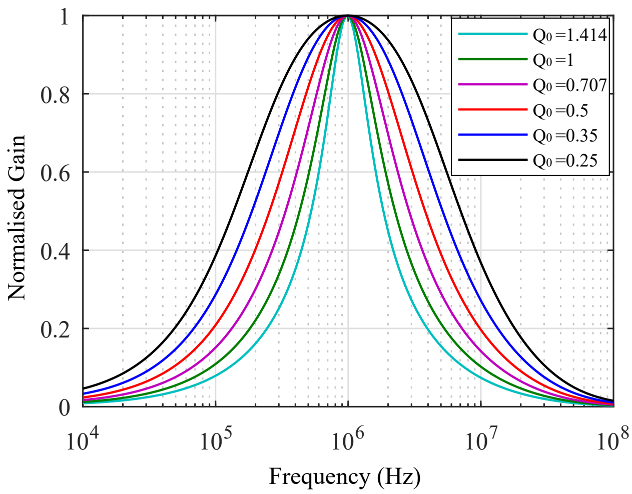


**Fig. 7:** $Q_0$ tunability with fixed center frequency at 1 MHz.

**Tab. 6:** Passive Components values for the tunability of the center frequency.

| Frequency (MHz) | 0.63 | 1 | 1.48 |
|---|---|---|---|
| $R_0$ (kΩ) | 5.72 | 3.6 | 2.45 |
| $R_1$ (kΩ) | 7.2 | 3.6 | 1.8 |
| $g_m$ (μA·V$^{-1}$) | 220 | 277 | 299 |
| $Q_0$ | 0.5 | 0.5 | 0.5 |

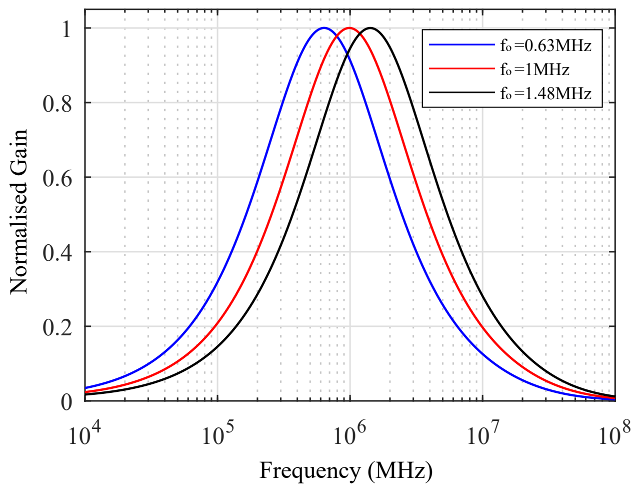


**Fig. 8:** Variation of center frequency with fixed $Q_0$.

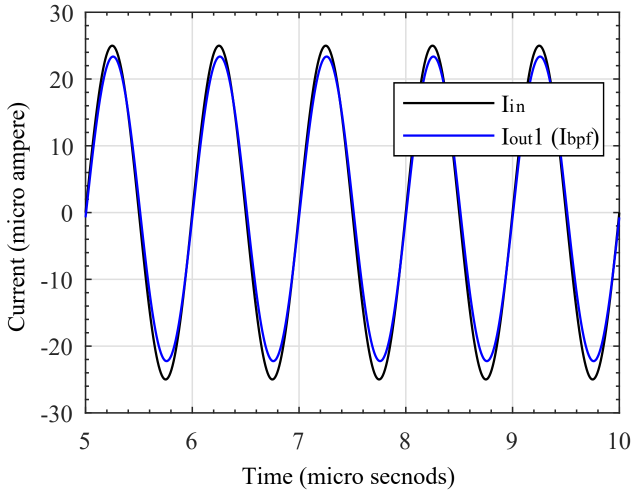


**Fig. 9:** Transient response of the band pass filter.

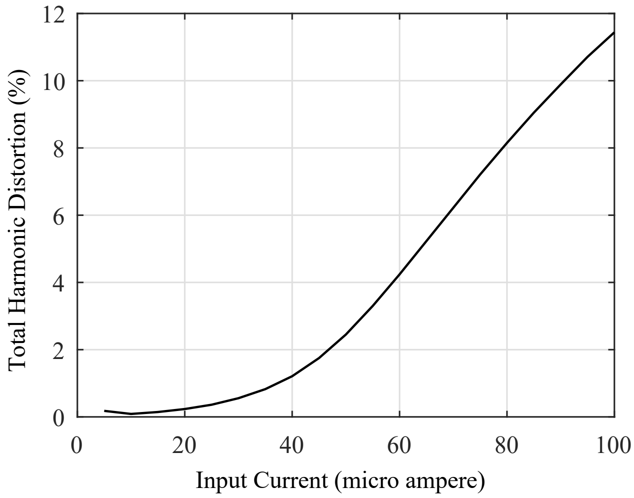


**Fig. 10:** THD curve for a band pass filter function.

ships. The measured phase angle is 88.3° and 89.4° respectively for Fig. 12 and Fig. 13.

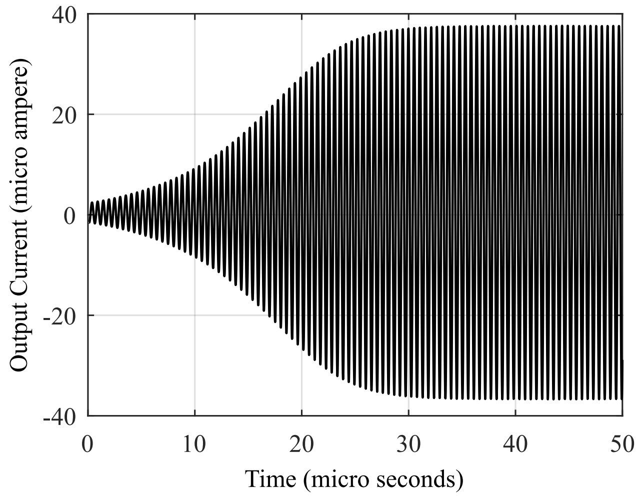


**Fig. 11:** Transient response of the current mode sinusoidal oscillator.

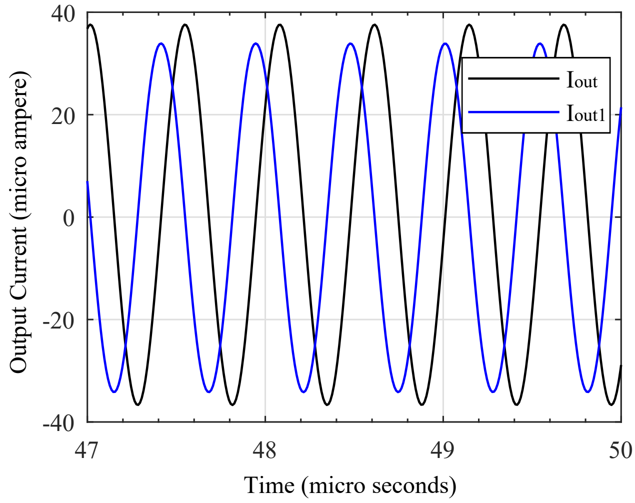


**Fig. 12:** Steady state response of the quadrature current outputs.

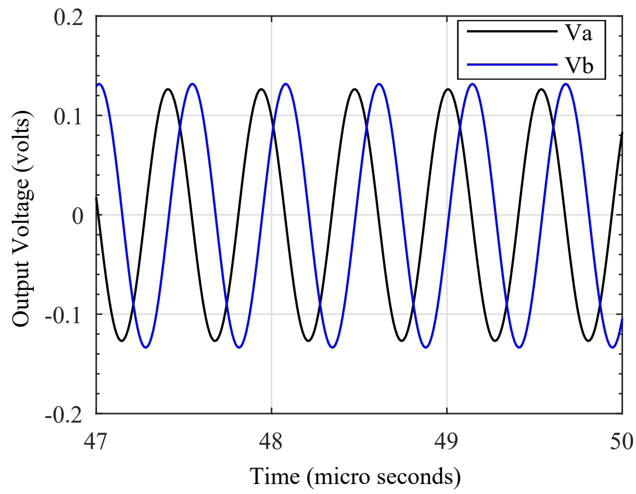


**Fig. 13:** Steady state response of the quadrature voltage outputs.

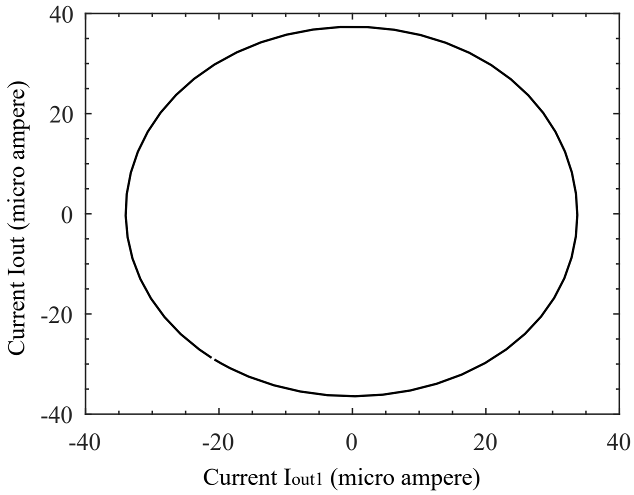


**Fig. 14:** Lissajous Pattern for current mode outputs.

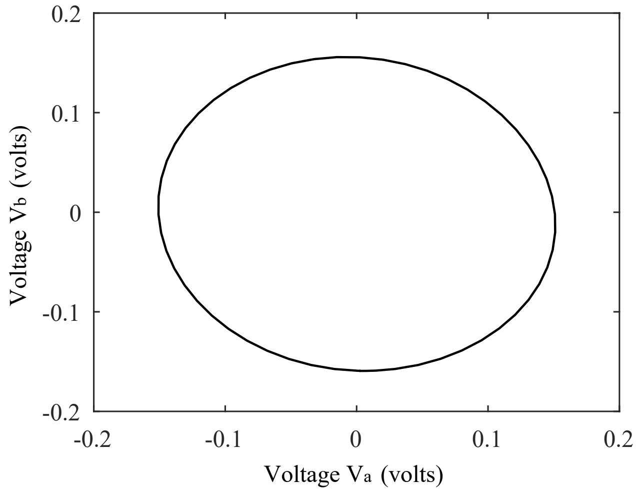


**Fig. 15:** Lissajous Pattern for voltage mode outputs.

The FFT representation of the explicit current output sinusoidal oscillator is shown in Fig. 16 (for better clarity and to see the availability of harmonics, y-axis has been taken in log domain). It is evident from Eq. (16) that the FO of the derived circuit can be varied with the help of grounded passive resistor i.e. $R_1$ and same can also be achieved by electronic tunability using $g_{m1}$. Figure 17 shows the variation of FO with respect to grounded resistor $R_1$ whereas Fig. 18 represents the electronic tunability of FO with respect to bias current of $g_{m1}$ i.e. $I_{B1}$. In Fig. 17, for the entire range of $R_1$ the FO is calculated and maximum error between simulated and calculated values of FO is found to be 6.78 % only. The variation of frequency, under the influence of parasitics, has also been computed. The values of parasitic elements ($R_X$ = 43 Ω, $R_Z$ = 362 kΩ, $R_N$ = 141 kΩ, $C_P = C_N$ = 0.92 pF) have been taken from [8]. In Fig. 18, for ideal frequency of 1.86 MHz (for $C_0 = C_1$ = 21.9 pF, $R_1$ = 3.6 kΩ and $g_{m1}$ = 236 μA·V$^{-1}$ at $I_{B1}$ of 35 μA) we get the simulated value as 1.84 MHz and including the effect of parasitic we get the FO 1.82 MHz with an error of 2.58 % with respect of ideal frequency.

The total harmonic distortion was also calculated for the entire usable range of the sinusoidal oscillator, as shown in Fig. 19. Figure 19 depicts that the THD is significantly low for the entire range of frequencies which strengthens the designed idea. However, the fluctuation presented in Fig. 19 can be reduced by introducing an additional AGC network as given in [20].

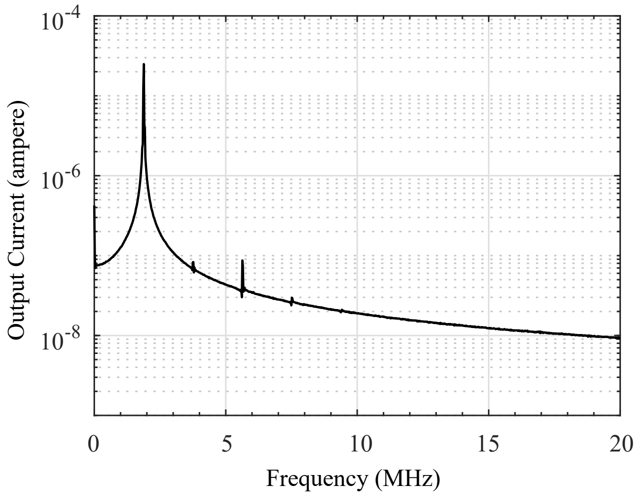


**Fig. 16:** FFT representation of the explicit current output of sinusoidal oscillator.

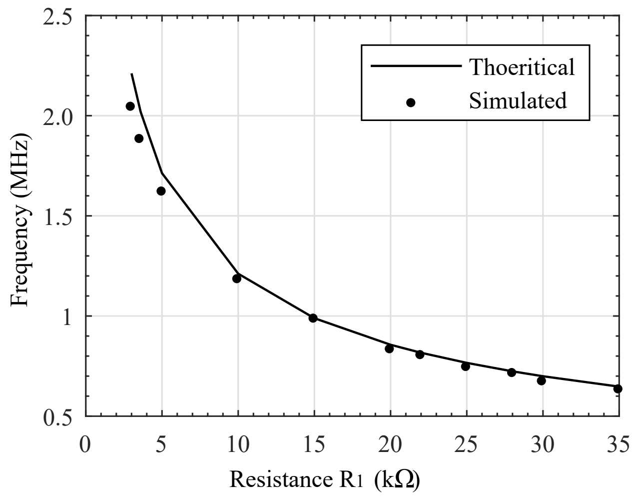


**Fig. 17:** Variation of FO with respect to a grounded resistor $R_1$.

## 6. Experimental Results

For practical implementation of VDCC as a block, a readily available integrated circuit i.e. OPA860 (see

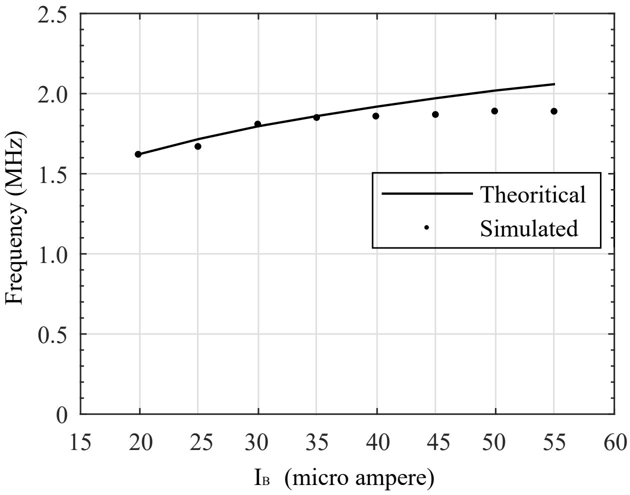


**Fig. 18:** Variation of FO with respect to the input bias current $I_{B1}$.

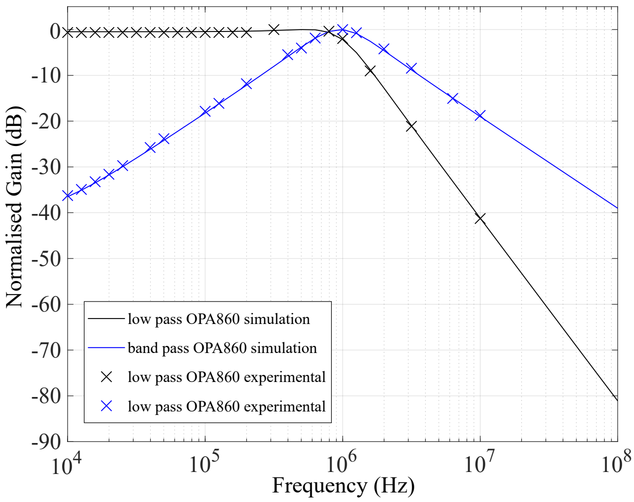


**Fig. 21:** Filter responses of low pass and band pass responses.

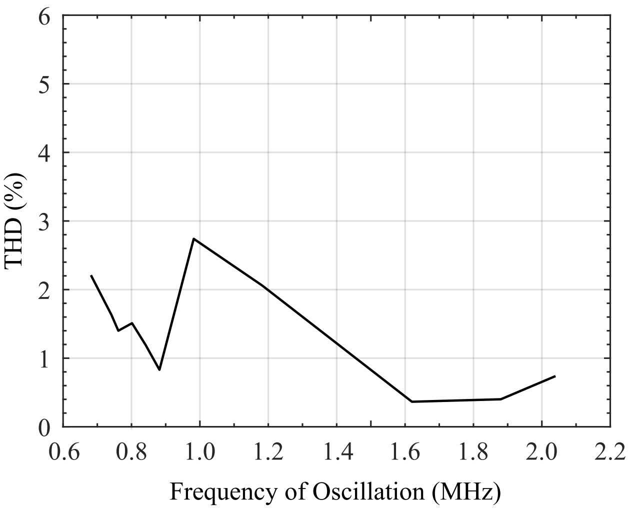


**Fig. 19:** Variation of FO with respect to calculated THD.

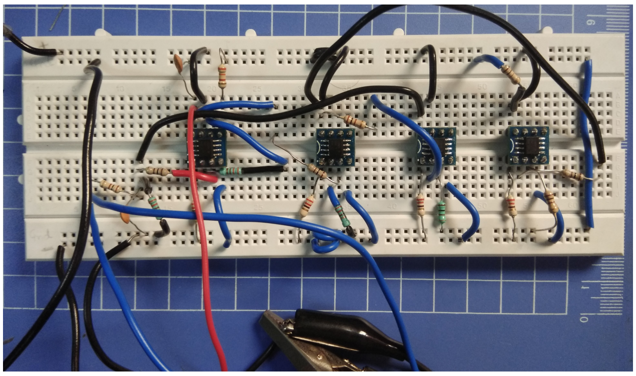

**Fig. 20:** Experimental setup for Active filter using VDCC.

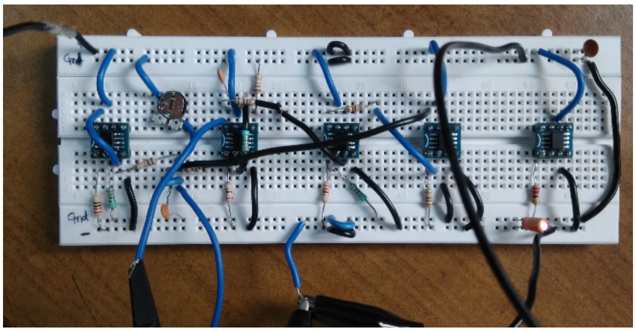

**Fig. 22:** Experimental setup for sinusoidal oscillator using VDCC.

Fig. 13 of [13]) have been used here. OPA860 is basically a diamond transistor [24]. Here it is worth mentioning that the resistors of 100 Ω are connected in series to the bases of OTA and buffers inputs [24]. The value of $R_{OFFSET}$ is also taken as 100 Ω (Fig. 13 of [13]).

For a generation of hardware results, we have used SCIENTIFIC Multiple power supply (PSD3304), SCIENTECH function generator (4061), SCIENTIFIC Oscilloscope (30 MHz, SM410). The passive component values, used in experimentation for the active filter, are $C_1 = C_2 = 470$ pF, $R_{m1} = 1/g_{m1} = 330$ Ω and $R_1 = R_0 = 330$ Ω. For the implementation of SRCO following passive elements have been taken, $C_1 = C_2 = 470$ pF, $R_{m1} = 1/g_{m1} = R_{m0} = 1/g_{m0} = 330$ Ω and $R_1 = 330$ Ω. Figure 20 and Fig. 22, respectively, shows the experimental setup for the active filter and sinusoidal oscillator using OPA860. The two (explicit) responses i.e. low pass and band pass are simulated using the PSPICE library file of OPA 860 obtained from `www.ti.com`. The results obtained are very much close to reality, as one can see in Fig. 21. For the purpose of experimentation low pass and band pass (explicit outputs, obtained experimentally) are also marked in Fig. 21. The frequency of operation was chosen as 1 MHz. Figure 23 shows the steady state quadrature output of the experimentally realized oscillator using OPA860. Here the frequency of operation is also chosen as 1.03 MHz (ideally) and the achieved frequency through simulation (using OPA860 macro model) is 935 kHz (with an error of 6.5 %). When the same is performed experimentally, the frequency of operation comes out to be 914 kHz (with an error of 2.2 % with respect to OPA860 simulation). To check the wide range of the oscillator, the graph between frequency of operation and a grounded passive resistor $R_1$ is plotted, shown in Fig. 24. The simulated and experimental values are in good agreement to each other.

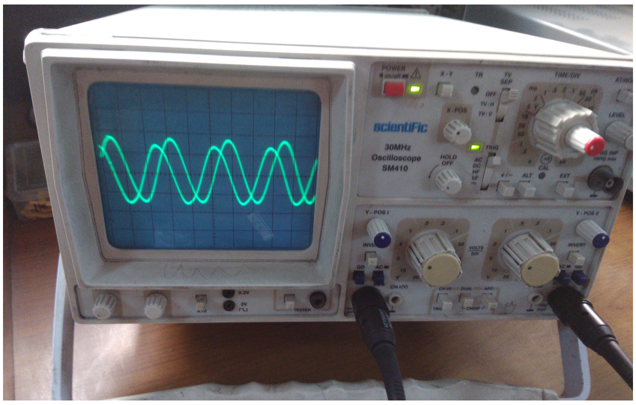

**Fig. 23:** Steady state output of the oscillator.

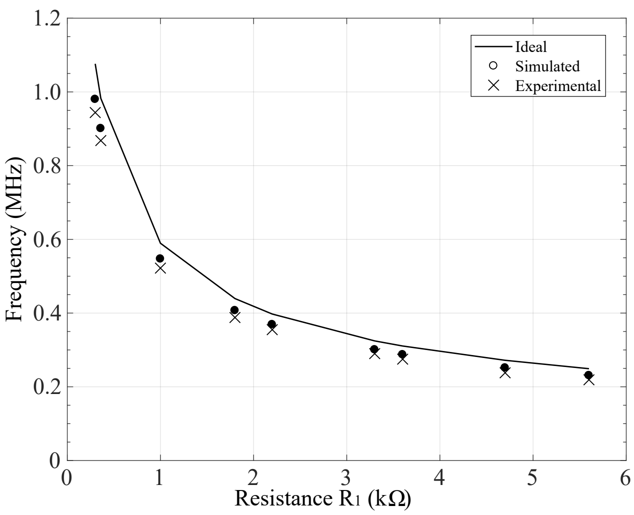


**Fig. 24:** Variation of FO with respect to a grounded resistor $R_1$.

## 7. Conclusion

This manuscript presents a realization of a current mode universal filter and a single resistance controlled oscillator successively, by altering the positions of the passive switches. Both the designed circuits employ only grounded passive elements and two active devices. Availability of explicit current outputs makes it a better proposition. The designed universal filter can produce all the five basic responses along with independent control of its quality factor. The derived SRCO has quadrature outputs in current mode (explicit output) as well as in voltage mode. The CO and FO of the oscillator are totally uncoupled and can be governed by a passive grounded resistor. The additional electronic tunability of CO and FO is also available. Regular mathematical analysis and typical simulation and experimental results justify the theoretical idea.

## Acknowledgment

All the experimental work was performed at Electronic Devices and Circuits Lab of the department of Electronics and Communication Engineering, Inderprastha Engineering College, Ghaziabad, Uttar Pradesh (India).

## References

[1] SENANI, R., D. R. BHASKAR and A. K. SINGH. *Current conveyors: variants, applications and hardware implementations*. New York: Springer, 2014. ISBN 978-3-319-08683-5.

[2] ARORA, T. S. and R. K. SHARMA. An all-mode KHN equivalent biquad using third generation current conveyor and all grounded passive elements. *Proceedings of the National Academy of Sciences, India Section A: Physical Sciences*. 2017, vol. 87, iss. 1, pp. 98–107. ISSN 0369-8203.

[3] SENANI, R., D. R. BHASKAR, M. GUPTA and A. K. SINGH. Canonic OTA-C sinusoidal oscillators: generation of new grounded-capacitor versions. *American Journal of Electrical and Electronic Engineering*. 2015, vol. 3, iss. 6, pp. 137–146. ISSN 2328-7365.

[4] ARORA, T. S. and R. K. SHARMA. A novel cubic generator realised by CCIII-based four quadrant analog multiplier and divider. *Indian Journal of Science and Technology*. 2016, vol. 9, iss. 38, pp. 1–8. ISSN 0974-6846. DOI: 10.17485/ijst/2016/v9i38/100026.

[5] PATHAK, J. K., A. K. SINGH and R. SENANI. New canonic lossy inductor using a single CDBA and its application. *International Journal of Electronics*. 2016, vol. 103, iss. 1 pp. 1–13. ISSN 0020-7217. DOI: 10.1080/00207217.2015.1020884.

[6] SENANI, R., D. R. BHASKAR, A. K. SINGH and R. K. SHARMA. *Sinusoidal oscillators and waveform generators using modern electronic circuit*

*building blocks*. Berlin: Springer. 2015. ISBN 978-3-319-23711-4.

[7] BIOLEK, D., R. SENANI, V. BIOLKOVA and Z. KOLKA. Active elements for analog signal processing: classification, review and new proposals. *Radioengineering*. 2008, vol. 17, iss. 4, pp. 15–32. ISSN 1210-2512.

[8] KACAR, F., A. YESIL, S. MINAEI and H. KUNTMAN. Positive/negative lossy/lossless grounded inductance simulators employing single VDCC and only two passive elements. *AEU-International Journal of Electronics and Communications*. 2014, vol. 68, iss. 1, pp. 73–78. ISSN 1434-8411. DOI: 10.1016/j.aeue.2013.08.020.

[9] JERABEK, J., R. SOTNER, R. PROKOP, V. KLEDROWETZ, A. KARTCI and U. E. AYTEN. Inductance simulator based on dual controlled CMOS voltage differencing current conveyor. In: *IEEE 59th International Midwest Symposium on Circuits and Systems (MWSCAS)*. Abu Dhabi: IEEE, 2016, pp. 16–19. ISBN 978-1-5090-0916-9. DOI: 10.1109/MWSCAS.2016.7870087.

[10] PRASAD, D. and J. AHMAD. New electronically-controllable lossless synthetic floating inductance circuit using single VDCC. *Circuits and Systems*. 2014, vol. 5, iss. 1, pp. 13–17. ISSN 2153-1285. DOI: 10.4236/cs.2014.51003.

[11] KARTCI, A., U. E. AYTEN, N. HERENCSAR, R. SOTNER, J. JERABEK and K. VRBA. Application possibilities of VDCC in general floating element simulator circuit. In: *European Conference on Circuit Theory and Design (ECCTD)*. Trondheim: IEEE, 2015, pp. 1–4. ISBN 978-1-4799-9877-7. DOI: 10.1109/ECCTD.2015.7300064.

[12] SRIVASTAVA, M., P. BHANJA and S. F. MIR. A new configuration for simulating passive elements in floating state employing VDCCs and grounded passive elements. *1st IEEE International Conference on Power Electronics, Intelligent Control and Energy Systems (ICPEICES-2016)*. Delhi: IEEE, 2016, pp. 1–4. ISBN 978-1-4673-8587-9. DOI: 10.1109/ICPEICES.2016.7853402.

[13] KACAR, F., A. YESIL and K. GURKAN. Design and experiment of VDDC-based voltage mode universal filter. *Indian Journal of Pure and Applied Physics*. 2015, vol. 53, iss. 5, pp. 341–349. ISSN 0975-1041.

[14] LAMUN, P., P. PHATSORNSIRI and U. TORTEANCHAI. Single VDCC-based current-mode universal biquadratic filter. In: *7th International Conference on Information Technology and Electrical Engineering (ICITEE)*. Chiang Mai: IEEE, 2015, pp. 122–125. ISBN 978-1-4673-7863-5. DOI: 10.1109/ICITEED.2015.7408926.

[15] RANA, S., A. K. KUMAWAT and P. KUMAR. A Universal current mode KHN biquad filter using voltage differencing current conveyor. In. *1st IEEE International Conference on Power Electronics, Intelligent Control and Energy Systems (ICPEICES-2016)*. Delhi: IEEE, 2016, pp. 3965–3970. ISBN 978-1-4673-8587-9. DOI: 10.1109/ICPEICES.2016.7853506.

[16] JAIN, R. and P. KUMAR. VDCC based voltage mode Tow-Thomas biquad filter. In: *1st IEEE International Conference on Power Electronics, Intelligent Control and Energy Systems (ICPEICES-2016)*. Delhi: IEEE, 2016, pp. 3971–3974. ISBN 978-1-4673-8587-9. DOI: 10.1109/ICPEICES.2016.7853464.

[17] SOTNER, R., N. HERENCSAR, J. JERABEK, K. VRBA, T. DOSTAL, W. JAIKLA and B. METIN. Novel first-order all-pass filter applications of z-copy voltage differencing current conveyor. *Indian Journal of Pure & Applied Physics (IJPAP)*. 2015, vol. 53, iss. 8, pp. 537–545. ISSN 0975-1041.

[18] PRASAD, D., D. R. BHASKAR and M. SRIVASTAVA. New single VDCC-based explicit current-mode SRCO employing all grounded passive components. *Electronics*. 2014, vol. 18, iss. 2, pp. 81–88. ISSN 2079-9292.

[19] SRIVASTAVA, M. and D. PRASAD. VDCC based dual-mode quadrature sinusoidal oscillator with outputs at appropriate impedance levels. *Advances in Electrical and Electronic Engineering*. 2016, vol. 14, no. 2, pp. 168–177. ISSN 1804-3119. DOI: 10.15598/aeee.v14i2.1611.

[20] SOTNER, R., J. JERABEK, J. PETRZELA, N. HERENCSAR, R. PROKOP and K. VRBA. Second-order simple multiphase oscillator using z-copy controlled-gain voltage differencing current conveyor. *Elektronika IR Elektrotechnika*. 2014, vol. 20, iss. 9, pp. 13–18. ISSN 1392-1215. DOI: 10.5755/j01.eee.20.9.8709.

[21] SOTNER, R., J. JERABEK, R. PROKOP and V. KLEDROWETZ. Simple CMOS voltage differencing current conveyor-based electronically tunable quadrature oscillator. *Electronics Letters*. 2016, vol. 52, iss. 12, pp. 1016–1018. ISSN 0013-5194.

[22] JERABEK, J., R. SOTNER, N. HERENCSAR, K. VRBA and T. DOSTAL. Behavioral model

for emulation of ZC-CG-VDCC. *IEICE Electronic Express*. 2016, vol. 13, iss. 18, pp. 1–6. ISSN 1349-2543. DOI: 10.1587/elex.13.20150859.

[23] MINAEI, S. and E. YUCE. Novel voltage-mode all-pass filter based on using DVCCs. *Circuits Systems and Signal Processing*. 2010, vol. 29, iss. 3, pp. 391–402. ISSN 1531-5878.

[24] OPA860-Wide bandwidth Operational Transconductance Amplifier (OTA) and Buffer. In: *National Instruments* [online]. Dallas: National Instruments, 2008. Available at: http://www.ti.com/lit/ds/sbos331c/sbos331c.pdf.

## About Authors

**Manish GUPTA** was born 1975 in Ghaziabad, Uttar Pradesh, India. He obtained B.Tech Degree in Electronics and Communication Engineering from Delhi College of Engineering, Delhi, (presently D.T.U. Delhi), M.Tech with specialization in Signal Processing from Netaji Subhas Institute of Technology, New Delhi and Ph.D. in area of Analog Integrated Circuits and Signal Processing from Jamia Millia Islamia, New Delhi, India. Currently he is working as an Associate Professor with Department of Electronics and Communication Engineering, Inderprastha Engineering College, Ghaziabad, Uttar Pradesh, India. His research interests are in the area of Bi-polar and CMOS, analog integrated circuits, current mode signal processing.

**Tajinder Singh ARORA** was born 1979 in Dehradun, Uttarakhand, India. He obtained B.Tech. Degree (Electronics and Communication Engineering) from Dehradun Institute of Technology, Dehradun, M.Tech. (Signal Processing) from Netaji Subhas Institute of Technology, New Delhi and Ph.D. (Analog Signal Processing) from Uttarakhand Technical University, Dehradun. He is currently working as an Associate Professor with Department of Electronics and Communication Engineering, Maharaja Surajmal Institute of Technology, New Delhi, India. His research interests are in the area of Analog and Digital signal processing He has authored or co-authored 20 research papers in International Journals and Conferences.